

Musical molecules: the molecular junction as an active component in audio distortion circuits

This content has been downloaded from IOPscience. Please scroll down to see the full text.

2016 J. Phys.: Condens. Matter 28 094011

(<http://iopscience.iop.org/0953-8984/28/9/094011>)

View [the table of contents for this issue](#), or go to the [journal homepage](#) for more

Download details:

IP Address: 129.128.50.162

This content was downloaded on 12/02/2016 at 15:21

Please note that [terms and conditions apply](#).

Musical molecules: the molecular junction as an active component in audio distortion circuits

Adam Johan Bergren¹, Lucas Zeer-Wanklyn^{1,3}, Mitchell Semple², Nikola Pekas¹, Bryan Szeto¹ and Richard L McCreery^{1,2}

¹ National Institute for Nanotechnology, Edmonton, AB, Canada

² University of Alberta, Edmonton, AB, Canada

³ University of Waterloo, Waterloo, ON, Canada

E-mail: adam.bergren@nrc.ca

Received 17 July 2015, revised 20 October 2015

Accepted for publication 21 October 2015

Published 12 February 2016



CrossMark

Abstract

Molecular junctions that have a non-linear current–voltage characteristic consistent with quantum mechanical tunneling are demonstrated as analog audio clipping elements in overdrive circuits widely used in electronic music, particularly with electric guitars. The performance of large-area molecular junctions fabricated at the wafer level is compared to currently standard semiconductor diode clippers, showing a difference in the sound character. The harmonic distributions resulting from the use of traditional and molecular clipping elements are reported and discussed, and differences in performance are noted that result from the underlying physics that controls the electronic properties of each clipping component. In addition, the ability to tune the sound using the molecular junction is demonstrated. Finally, the hybrid circuit is compared to an overdriven tube amplifier, which has been the standard reference electric guitar clipped tone for over 60 years. In order to investigate the feasibility of manufacturing molecular junctions for use in commercial applications, devices are fabricated using a low-density format at the wafer level, where 38 dies per wafer, each containing two molecular junctions, are made with exceptional non-shorted yield (99.4%, representing 718 out of 722 tested devices) without requiring clean room facilities.

Keywords: molecular electronics, clipping, audio, distortion, guitar

 Online supplementary data available from stacks.iop.org/JPhysCM/28/094011/mmedia

(Some figures may appear in colour only in the online journal)

1. Introduction

Molecular electronics is a field of study that investigates the use of organic molecules as circuit elements in which the length of the current path is of molecular dimensions, generally 1–10 nm. In 2014, molecular electronics celebrated [1] 40 years since a landmark theoretical paper [2] that is often correlated with the origin of the field. During the four decades since, numerous studies have intended to determine the ‘rules’ that dictate molecular electronic device properties [3, 4]. The molecular junction (MJ), which can contain a single molecule or many billions

of molecules oriented in parallel between two conductors (see figure 1(A)), is the foundational unit in molecular electronics and has been studied in many different configurations [5]. These studies have advanced the understanding of charge transport mechanisms in MJs [6, 7], and have also led to a refined ability to fabricate reliable, robust, and reproducible MJs [8, 9].

Motivations often cited for molecular electronics include very large scale integration [10], improvement of extant semiconductor device performance metrics for functions such as logic [11], memory [12, 13], rectification [14–16], and negative differential resistance [17], and even totally new functions not possible

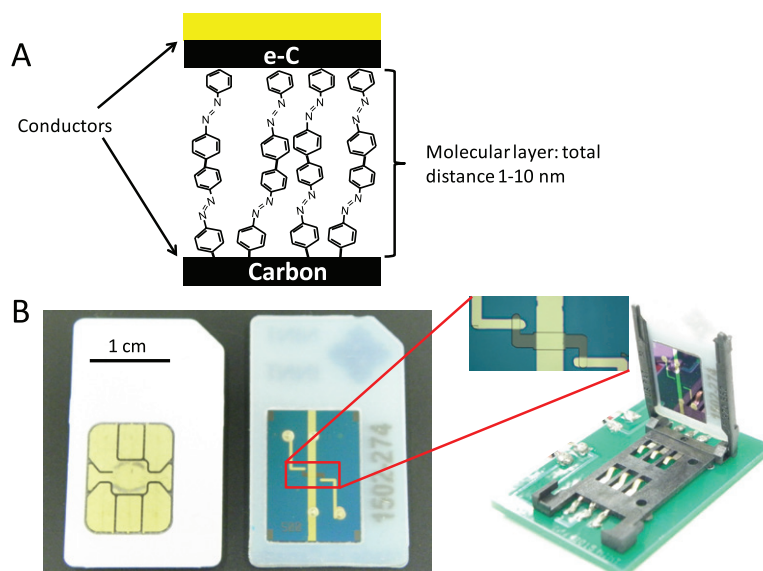


Figure 1. (A) Cross-sectional schematic of an idealized molecular junction structure, showing organic molecules sandwiched between two conducting contacts, in this case consisting of a carbon bottom contact and electron-beam evaporated carbon (10 nm) and Au (100 nm) as the top contact. (B) Photograph of the molecular junctions fabricated using a SIM-card pin-out (with a conventional SIM card shown for comparison) to simplify testing and integration into analog circuits, as shown at right. Junction area is $\sim 10^{-4} \text{ cm}^2$.

with conventional semiconductor electronics [18]. Research into all of these areas continues to play an important role in shaping the future of molecular electronics. Here, we present an application of a large-area MJ that has immediate practical value as a discrete component in analog audio clipping circuits. Traditional audio clipping circuits often utilize electronic components with non-linear current–voltage properties (e.g. pn junction diodes) to shape signal waveforms and add distortion. We demonstrate that molecular devices have unique and tunable non-linear electronic properties due to the distinct nature of charge transport involved in nanoscale devices relative to bulk semiconductor junctions, where both the size scale and materials of the active part of the devices are dissimilar. The electronic properties of molecular junctions resulting from these differences lead to a unique sound character when employed in analog clipping circuits that has not been achieved with conventional semiconductors, despite more than four decades of effort for such circuits to replace the tube-based amplification currently prevalent for electric guitars. Importantly, the parameters that affect the electronic properties of the MJ (e.g. molecular layer thickness) can be controlled to fine-tune performance and musical quality.

After demonstrating the application of MJs in audio clipping circuits, we discuss junction fabrication techniques that are amenable to manufacturing and integration with conventional circuitry. These methods are relatively simple in that no specialized clean room facilities are required. In addition, the tight distribution of conductance achieved with the reported technique serves to validate molecular junctions as manufacturable technology, as well as achieving statistical validation of charge transport measurements.

2. Experimental

The MJs used here are composed of carbon/molecule/carbon [9] layers arranged in a cross junction format, as shown in

figure 1(A). The molecular layer is grown electrochemically on the bottom carbon electrode, enabling reliable control of the thickness in the nanometer range and the resulting electronic properties. A detailed description of the junction fabrication methods and results will be given later, along with analysis of yield and reproducibility. It is important to note that the idealized diagram in figure 1(A) does not represent the degree of disorder in the molecular layers. However, as previously discussed [5], the strong chemical bonding resulting from diazonium reduction yields increased stability at a cost of reduced order. This trade-off is especially important for the practical application discussed in this paper. Figure 1(B) shows photographs of a molecular junction made to match the pin-out of a SIM-card holder (a conventional SIM card is shown at left). Figure 1(B) also shows a molecular device mounted into a 3D printed adapter for a SIM-card holder (Amphenol-Tuchel Electronics P/N C707 10M006 5002, DigiKey P/N 361-1020-2-ND), illustrating the electronic connections to external circuitry.

Current–voltage curves were obtained using a Keithley 2602A source-measurement unit, a Gamry reference 600 potentiostat, or a custom-built LabVIEW measurement system that has been described elsewhere [19]. Audio-frequency voltage signals were generated using a National Instruments 5421 arbitrary waveform generator with 50Ω output impedance and sent to the input of the prototype clipping circuit which is described in detail in the online supporting information (stacks.iop.org/JPhysCM/28/094011/mmedia). The output signal from the prototype was digitized using a PreSonus AudioBox USB with 24-bit resolution at a sampling rate of 48 kHz. This digital signal was captured via a modified LabVIEW program [20] that enabled the resultant waveform and the power spectrum to be directly observed and exported. The FFT power spectrum function within LabVIEW was utilized to capture the harmonic spectrum, with 100 RMS averages used to reduce noise.

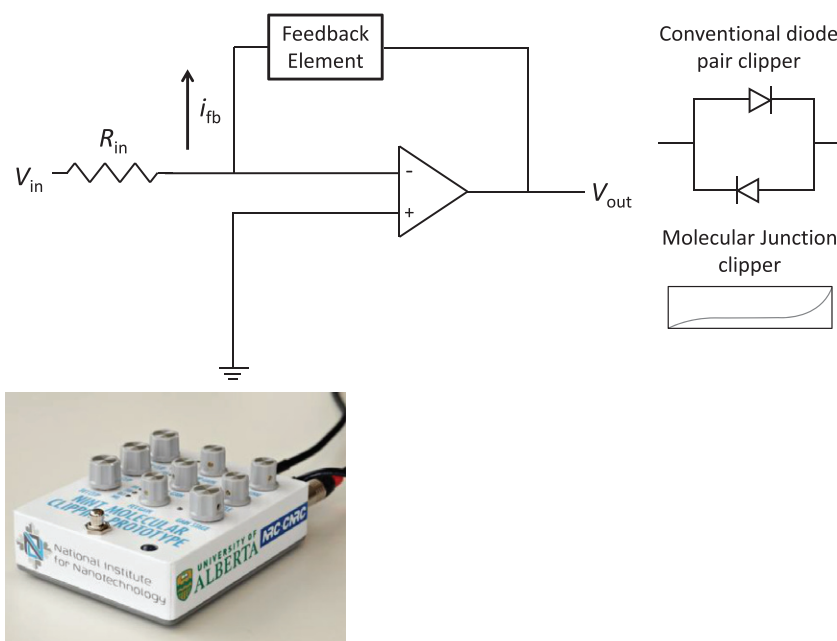


Figure 2. Simplified schematic showing the clipping amplifier section of the circuit employed in the prototype for the op-amp clipping gain stage (traditional clipping diode pair shown at right, along with a proposed electronic symbol for a molecular junction. The photograph at bottom shows the actual prototype built by Dr Scientist Sounds, a Canadian effects maker. The full schematic is shown in the online supporting information (stacks.iop.org/JPhysCM/28/094011/mmedia).

3. Results and discussion

Analog circuitry is normally designed to avoid distortion of the input signal so that an electronic function can be performed with minimal artefacts or loss of fidelity. In many technical applications, the accuracy of an electronic signal is critical, with distortion resulting in lost or obscured representations of source information. On the other hand, certain intentional distortions or artefacts have been employed as a tool for artistic expression. For example, many image processing software packages include algorithms to simulate film grain or soft focus, thereby adding a distorting effect that can be aesthetically pleasing. In the case of sound, the history of electronic instrument amplification, along with the popularity of certain forms of music, has led to a complex array of techniques for altering electronic signals, including intentionally distorting audio signals to yield increased sound complexity.

In the case of electric guitar, analog circuits that are specifically designed to introduce distortion have been used since the 1960s [21]. Part of the reason for the prevalence of distortion in guitar-based music stems from the distortion generated from overloading tube amplifiers, which were initially the only available amplification devices for electric guitars. While the original goal of tube amplifier design was to accurately reproduce the electric guitar signal with a simple increase in volume (often termed ‘clean’ amplification), the technical limitations of tube amplification led to clipping of the audio signal that is increasingly apparent at higher volumes (see the online supporting information (stacks.iop.org/JPhysCM/28/094011/mmedia)). Clipping results when the conditions used to amplify a signal place a demand on the amplifier to produce more output signal than it is designed

to deliver, leading the signal extremities (i.e. the peaks and troughs of a waveform) to be clipped, producing a waveform that has a different shape than the input signal. Such time-domain clipping leads to addition of harmonics in the frequency domain, increasing perceived complexity. Tube amplifier clipping became known as ‘overdrive’, and as early as the 1950s provided guitarists with a unique sound that played a major role in the foundation of Rock and Roll. Distorted tones of guitars and other instruments continue to be used across many modern musical genres, with a wide variety of methods used to distort the sound. These methods often involve audio signal processing circuits based on tube [22, 23], analog [21], and digital technologies [24] designed to emulate different conditions of tube amplifier overdrive as well as other distorting effects (e.g. broken speakers). These different sound qualities form a ‘timbre toolbox’ for the musician to use in different contexts.

A particularly common analog distortion circuit that utilizes voltage waveform clipping as its operational basis is shown in figure 2. Here, the operational amplifier is used within its normal functioning limit to shape the input voltage signal from the guitar through feedback, where one of the amplifier inputs is connected to its output so that the resulting signal represents a clipped waveform (typical signals from passive electric guitar pickups have amplitudes of ~ 100 mV; see the online supporting information (stacks.iop.org/JPhysCM/28/094011/mmedia)). Such feedback clipping forms the heart of many ‘analog overdrive’ effects. Feedback clipping works to shape the signal using a feedback component with a non-linear current–voltage function. For the case of the op-amp circuit shown in figure 2, the amplifier is set up to demand a particular current given by the ratio of the input

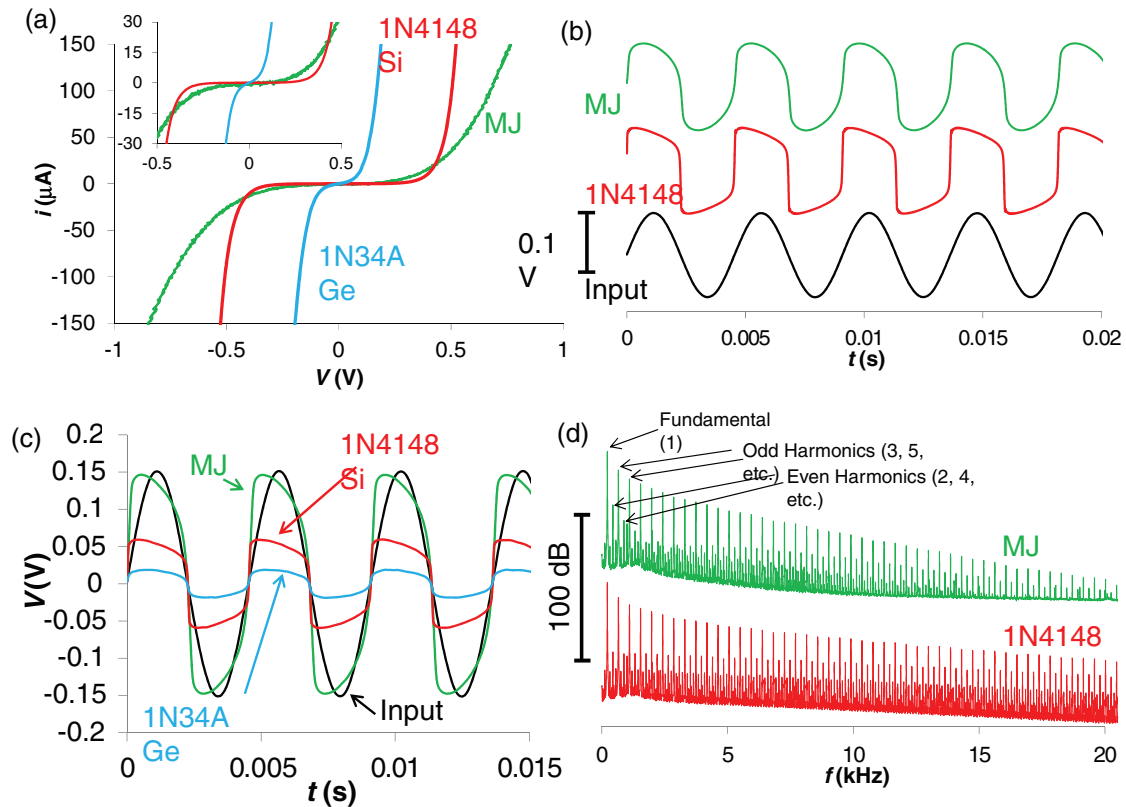


Figure 3. (A) i - V curves of a ~ 5 nm azobenzene molecular junction (green curve) and conventional clipping diode pairs (Si, red curve; Ge, blue curve). (B) The input sine wave (black curve) is shown below the output resulting from using the MJ clipper (green curve) or diode pair clipper (red curve), where the output was scaled to match the input amplitude. (C) Shows the resulting waveforms for input, MJ clipper (green), Si diode pair clipper (red), and Ge diode pair clipper (blue), where the amplitude results from the clipping device characteristics shown in (A). (D) The power spectra for the Si and MJ waveforms in (B) with odd and even harmonics labeled.

voltage (V_{in}) to the input resistor (R_{in}) through Ohm's law. The total current, defined by V_{in}/R_{in} , will flow through the feedback loop (i_{fb}), and this value of current corresponds to a particular output voltage (V_{out}) based on the feedback clipper's voltage at i_{fb} . Thus, the shape of the output voltage waveform is dictated in large part by the specific current-voltage relationship of the feedback element. This is due to the fact that the output voltage for each input voltage is determined by the current-voltage curve of the feedback clipper such that as the input voltage increases, the output voltage will trace the current-voltage curve of the feedback element. For the case of the diode clippers, the resulting output voltage waveform will then take a fairly sharp shape since the output voltage will suddenly rise from near zero (for low input voltages, which give small current demands) to nearly maximum output when the diode on voltage is reached. A molecular junction, on the other hand, results in a slow onset of the output voltage since there will be a larger voltage range associated with small currents, giving larger output voltages at moderate current draw (which correlates with the initial rise time of the waveform). While this description does not consider other important factors, such as the specific properties of circuit components (i.e. the frequency response of the op-amp or the presence of pre-clipping filters), it does encompass the main changes that act to alter the sound when *only* the feedback element is changed in a particular analog overdrive circuit. In order to determine how molecular junctions perform in feedback

clipping circuits, a demonstration prototype was constructed (see figure 2 and the online supporting information (stacks.iop.org/JPhysCM/28/094011/mmedia)) that contains a feedback clipping circuit as well as other clipping circuits.

Figure 3(A) shows the electronic properties of three different feedback elements: two different 'head-to-toe' diode pairs that are often used in clipping circuits (1N4148 Si, red curve; 1N34A Ge, blue curve) and an MJ (green curve). The prototype circuit was set to demand a peak i_{fb} of $75 \mu\text{A}$ for the test conditions employed ($V_{in} = 0.15 \text{ V}$ peak-to-peak at 220 Hz and $R_{in} = 2 \text{ k}\Omega$). In the context of the circuit shown in figure 2, analysis of the current-voltage curves in figure 3(A) indicates that the MJ is expected to have a more rounded wave shape than when Si diodes are used due to the more gradual onset of current with increasing voltage. Figure 3(B), which shows the output of the feedback clipping circuit, shows that this is indeed the case. The output signals in figure 3(B) were adjusted to match the input voltage through a post-clipping stage volume control. In order to show how the clipping element impacts output amplitude, a similar test was carried out without scaling output voltage. Figure 3(C) shows waveforms that demonstrate when V at i_{fb} (here $\sim 75 \mu\text{A}$) is smaller (see figure 3(A)), the output amplitude is smaller. Thus, the use of Ge diodes (which have very small voltages associated with currents up to $75 \mu\text{A}$ due to their low on voltage) for clipping results in the lowest amplitude, with Si diodes next, followed by the MJ, since V at i_{fb} is 0.15 V , 0.49 V , and 0.62 V , for Ge, Si

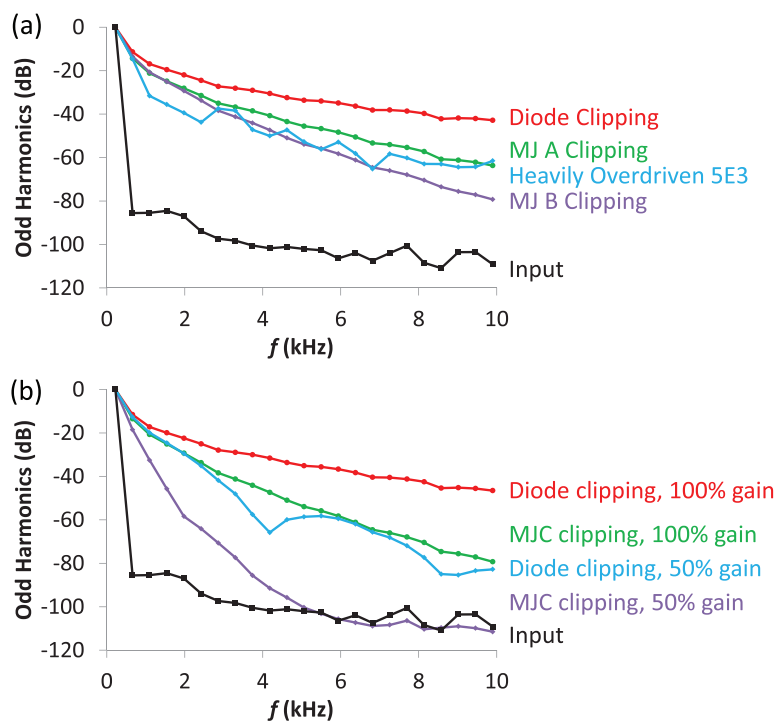


Figure 4. (A) Comparison of frequency distribution resulting from clipping via tube amplifier overdrive (blue curve) and the op-amp overdrive circuit using silicon diodes (red curve) and two different MJs (green and purple curves) clippers. (B) Comparison of power spectrum envelopes for diode clipping and molecular junction clipping for different levels of ‘gain’ showing the ability to tune into a wide range of harmonic saturation with the MJ clipper. The input trace (black curve) in both cases shows the noise floor of the measurement electronics.

and MJ devices, respectively. This illustrates that the molecular devices, in comparison with diode pairs, can provide a steeper roll-off of high frequencies without compromising the dynamic range of the signal amplitude.

Power spectra for the clipped waveforms in figure 3(B) are shown in figure 3(D), which permits comparison of sound quality of different circuits through their effects on the distribution of harmonics. The Si diode clippers produce a harmonic envelope with more prevalent high frequency content, while the MJ provides less prominent higher frequencies, resulting in a generally ‘warmer’ perceived tone. Although sound quality is always subjective and listener-dependent, power spectra provide objective evidence of how the electronics modify the distribution of harmonics, and permit comparison of new circuits to current devices with wide popular appeal. In order to more directly visualize and compare power spectra, the envelopes of the odd and/or even harmonics can be plotted as a function of frequency for different clipping devices, as discussed below.

Figure 4(A) shows the power spectrum envelope for odd integer harmonics for several cases (for further discussion of odd and even harmonics, see the online supporting information (stacks.iop.org/JPhysCM/28/094011/mmedia)) where the frequency range is restricted to 10kHz to allow closer inspection of the differences. Analysis of figure 4(A) shows that measurable differences result when processing the signal with different clipping circuits. First, it is clear that diode clipping results in the most prominent odd harmonic presence, particularly at high frequencies. Second, two different molecular junctions, containing different molecular

layer thicknesses (green and orange curves), yield different levels of harmonic distortion. In this case, the conductance of MJA is ~ 4 times higher than MJB at 0.5 V. By considering the attenuation factor (β), which is defined as the negative value of slope of a plot of the natural logarithm of current as a function of distance, we can calculate the thickness difference that is consistent with these data. Since the value of β is characteristic for particular molecule and contact systems, we used here the previously measured value for the carbon/molecule/carbon devices used in this paper, which was reported [9] to be 3.3 nm^{-1} . Thus, MJA is calculated to be $\sim 0.4 \text{ nm}$ thinner than MJB. Consideration of these data, along with the exponential conductance-thickness relationship established in these molecular electronic devices [9, 25, 26], shows that it is possible to tune the clipped sound of an analog overdrive circuit over a wide range by a simple change in the molecular junction, as illustrated by the measurable difference resulting from a $\sim 0.5 \text{ nm}$ change in molecular layer thickness. Third, comparison with an overdriven tube amplifier (blue curve) shows that the use of MJs in the prototype most closely yields an odd-harmonic distortion response similar to an overloaded tube amplifier. The tube amplifier used for this comparison was designed in 1955, and is still manufactured and sold on a large scale today, illustrating the desirability of the sound of tube clipping in guitar music (see the online supporting information for further comparisons with a more modern tube amplifier (stacks.iop.org/JPhysCM/28/094011/mmedia)). Taken together, it is clear from figure 4(A) that MJs provide a softer clipping character than diodes in the same circuit, and that the properties of the MJ can be tuned by changing the structure

(here, thickness) to control the harmonic spectrum, and that the odd harmonic spectra resulting from the use of either MJ in the overdrive circuit more closely approach tube clipping than diode clippers.

In addition to providing a more ‘tube-like’ harmonic distribution than diodes, MJs also result in less attenuation of the signal due to the more gradual onset of current at lower voltages. To show how this more limited reduction in voltage amplitude during clipping results in increased dynamic range, we plot in figure 4(B) the odd harmonic envelope for the prototype op-amp overdrive circuit where different levels of current are sent through the feedback clipping component by reducing the gain knob on the prototype (see the online supporting information (stacks.iop.org/JPhysCM/28/094011/mmedia)). It is clear that between 50% and 100% on the gain potentiometer results in a much smaller effect on harmonics for diode clippers than for the molecular junction. This is due to the fact that molecular junctions have a more gradual onset at low voltage (i.e. they do not have an ‘off’ state) as well as a lower ratio of the high/low conductance states (see i - V curves in figure 3). In other words, the pn junction diodes turn on suddenly at their forward voltage (V_f), going from resistances of ~ 1 M Ω , to a few tens of Ohms at V_f , while an MJ operates via a tunneling mechanism that gives low voltage resistances of 100s of k Ω and high voltage resistances of a few k Ω . Not only does this mean that diodes have a harder clipping character (characterized by a more squared-off waveform as shown in figure 3(B)), but it also limits the dynamic range of clipping. By comparison, the range of clipping for MJs can be tuned more broadly, as illustrated in figure 4(B).

In order to demonstrate how the differing physical principles of MJs and pn diodes affect their current–voltage behavior, consider the functional forms of current–voltage curves for each device. For the pn junction, the Shockley equation [27] describes the current–voltage relationship for an ideal diode:

$$i = i_0 \left(e^{\frac{V}{nkT}} - 1 \right), \quad (1)$$

where i is the current, i_0 is the saturation current, V is the voltage, n is the ideality factor, k is the Boltzmann constant (8.62×10^{-5} eV K $^{-1}$), and T is temperature in Kelvin. The geometric factors and other underlying physical phenomena that lead to this treatment can be found in Sze’s comprehensive text on semiconductor physics [27]. The current–voltage curves for molecular junctions and their dependence on temperature and molecular layer thickness are consistent with quantum mechanical tunneling [8, 28]. For the molecular junctions used here, a Simmons model treatment that includes image charge corrections of the effective barrier height and width [25] adequately describes the current–voltage behavior, with the mathematical details available elsewhere [25]. In brief, the current through a tunnel junction is exponentially dependent on the thickness of the molecular layer and the barrier height (i.e. the energy difference between the Fermi level and the molecular orbital(s) that mediate transport). Figure 5(A) shows a calculated current–voltage curve for a pn diode compared to those for molecular junctions with molecular layer thickness from 2.2 to 5.2 nm. It is clear that these models, which are based

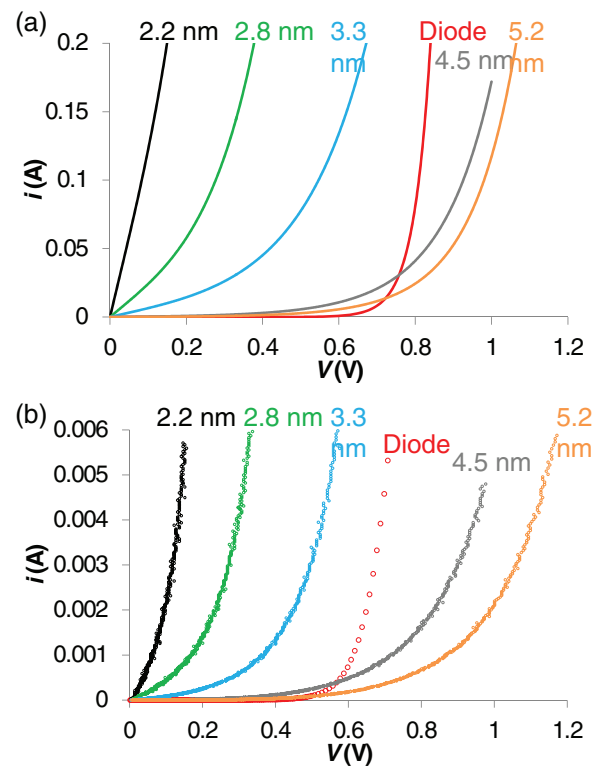


Figure 5. (A) The mathematically predicted electronic properties of a 1N4148 diode (red curve) compared to a series of molecular junctions with different thicknesses (black, green, blue, grey, and orange curves). The diode was fit using the Shockley equation (with $n = 1.7$, and $i_0 = 1$ nA), while the simulation data for the molecular devices were taken from [25]. (B) The electronic properties, represented as the current–voltage curve for molecular junctions containing a variety of molecular layer thicknesses (data taken previously published in [25]) overlaid against the response of a 1N4148 Si diode.

on different transport mechanisms, produce quite different results, where the molecular junctions show a more gradual onset of current with voltage, and where the range of electronic response can be changed to a significant extent by variation of thickness. For comparison, figure 5(B) shows an overlay of previously reported experimental data for a series of molecular devices and a diode [25]. Here, the same trends are observed as for the simulated electronic properties shown in figure 5(A). The distinct character of the MJ tunnel junction and the conventional pn junction in clipping circuits results from different underlying physics, and results not only in distinct ‘sounds’ but also the ability to vary the harmonic distribution by changes in molecular layer thickness.

The attractions of molecular junctions compared to conventional diodes in audio circuits stimulated consideration of commercial production of molecular junctions, including scaled-up fabrication with high yield and reproducibility. There are numerous platforms for making molecular junctions, ranging from large area to single molecule devices [5, 18]. In the case of large area molecular electronic junctions used here, most commonly a bottom-up fabrication methodology has been used, including up-scaled approaches [29]. However, the application of a molecular junction in a real-world circuit requires that two demands be met: (1) the MJ

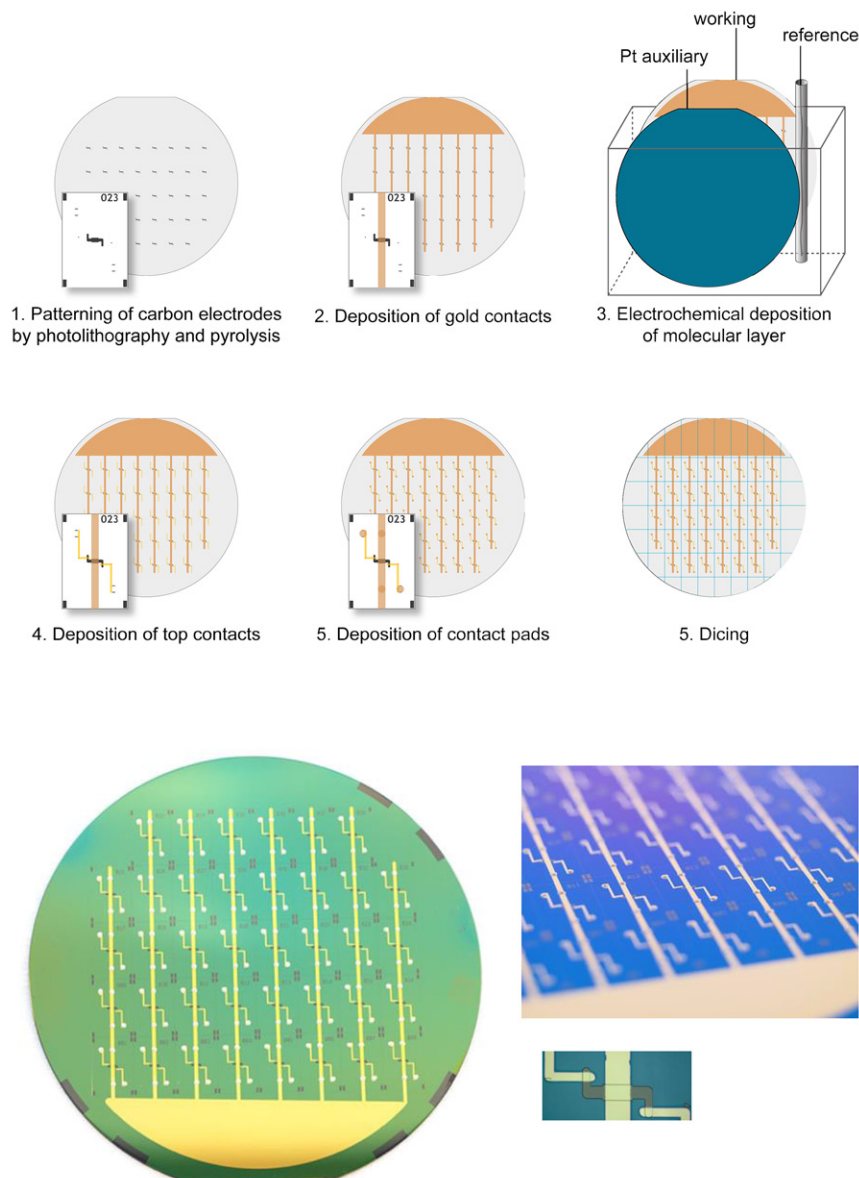


Figure 6. Top: wafer scale fabrication flow diagram. Starting with a 4 inch wafer, carbon is deposited, followed by metallic lines used to make contact for electrochemical molecular layer deposition. Finally, top contacts are deposited, followed by contact pads. Bottom: photograph of a finished wafer, complete with Ag epoxy bumps to ensure reliable connection when mounted in the SIM card holder.

must be manufacturable through a process that is compatible with the requirements of integration and packaging (particularly parallel fabrication and packaging in a format that allows easy connection); and (2) the MJ itself must withstand continuous operational temperatures, voltages, and corresponding currents. We have previously shown [9, 25] that a molecular junction made on carbon substrates, with molecular layers deposited via electrochemical reduction of aromatic diazonium salts and top contacts of copper [25] or carbon [9] can withstand long-term voltage cycling. We have also shown that such devices can be microfabricated [19] and subjected to high temperatures and wet processing for microelectronic production and packaging [30]. Here, we present a scalable fabrication approach using 100 mm wafers that produce

molecular device chips in the form of a mini SIM-card (see figure 1). Figure 6 shows a process flow diagram used to fabricate 38 dies per wafer, each with 2 molecular devices. In brief, silicon wafers with a 300 nm thick layer of thermal oxide were cleaned with piranha (*warning: piranha is highly reactive!*). After cleaning, photoresist (AZ 4330) was spun onto each wafer using a Site Services SpinBall Coater with a program consisting of spinning at 500 rpm for 10 s to spread, and 2500 rpm for 35 s to coat, followed by a soft bake at 110 °C for 180 s (resulting film thickness $\sim 5 \mu\text{m}$). Photolithography was carried out using a Quintel 4000 contact aligner with a UV exposure of 20 s (intensity 17.7 mW cm^{-2} at 405 nm and 8 mW cm^{-2} at 365 nm) with subsequent development in a 1 : 3 dilution of AZ developer:water. After photolithography,

Table 1. Summary of conductance, yield, and reproducibility for molecular devices.

Wafer	i_{avg} @ 1 V (mA)	RSD @ 1 V	Notes
D1	500 ± 100	20%	
D2	765 ± 170	22%	
D4	445 ± 107	24%	
D5	493 ± 114	23%	Excludes 1 short circuit
D6	403 ± 142	35%	
Total run (single sample)	562 ± 182	32.4%	Excludes 1 short circuit
	Devices	% Yield	
Total yield, run D	188/189	99.5%	non-shorted
Application yield, run D	186/189	98.4%	Produces stable and useful clipping
Total yield, 4 runs	718/722	99.4%	non-shorted
Application yield, 4 runs	472/494	95.5%	Produces stable and useful clipping

wafers with photoresist features were pyrolyzed in a 5 inch tube furnace by heating under a constant ~1500 sccm (tube diameter is 5 inches) flow of forming gas (5% H₂, balance N₂) to 1050 °C at 10 °C per minute. The temperature was held at 1050 °C for 1 h before cooling down to room temperature in flowing forming gas. The process of pyrolysis, as discussed previously [31], converts the photoresist to a form of conducting carbon similar in some properties to glassy carbon, but with a very smooth surface with RMS roughness of less than 0.5 nm [31, 32]. The low roughness and absence of grain boundaries enables reproducible molecular layers of 2–6 nm thickness to be grown on the surface.

Before the molecular layers are grown on carbon electrodes using the electrochemical reduction of diazonium reagents, an electrical connection to individual carbon electrodes is realized simultaneously by electron-beam deposited pattern of Cr (5 nm) and Au (100 nm) through wafer-sized shadow masks (see figure 6). A conventional three electrode electrochemical cell was then used to grow molecular layers on pyrolyzed photoresist features as the working electrode, a Ag/Ag⁺ reference electrode and a wafer-sized Pt auxiliary electrode made through electron-beam deposition of Cr(10 nm) and Pt(300 nm) on a Si/SiO_x wafer. The molecular layer was deposited by sweeping the voltage from 0.4 V to –0.6 V (versus Ag/Ag⁺) at 0.2 V s^{–1} in a 1 mM azobenzene diazonium ion solution in acetonitrile with 0.1 M tetrabutylammonium tetrafluoroborate as supporting electrolyte [25]. Between 1 and 5 voltammetric cycles were used to vary the molecular layer thickness, verified by atomic force microscopy [33]. After rinsing and drying the modified PPF electrodes, top contacts were deposited by electron-beam evaporation of 10 nm carbon from graphite rods, followed by 100 nm of gold (see figure 6) [9].

Once the wafers with devices are complete, *i*–*V* curves of several randomly selected junctions were recorded to ensure that the molecular junctions were intact and non-shorted. For wafers that pass spot-checking, electron beam deposition of 5 nm Cr and 100 nm Au circular dots was carried out using a shadow mask with a pattern that matches the pin-out of a SIM card holder (Amphenol-Tuchel Electronics P/N C707 10M006 5002, DigiKey P/N 361-1020-2-ND). These dots facilitate the subsequent deposition of Ag epoxy (EpoTek H20E) on four spots on each die in order to ensure good electrical contact

between the molecular device and the SIM-card pins (see figure 1). After curing of the silver epoxy for 1 h at 100 °C, the *i*–*V* curves for one device on every die on the entire wafer were obtained.

To illustrate the effectiveness of this fabrication method, we summarize the results from four runs of six wafers each, as well as from the behavior of five working wafers from a single run. Overall, in four runs, 19 out of 24 wafers produced working devices. In the case of the five non-working wafers, the failure correlated to loss of potential control during the electrochemical deposition such that no molecular layer resulted from electrochemical scanning. Post-analysis revealed the likely cause to be the electrolysis solution creeping onto the copper alligator clips, which produces undesired electrochemical reactions, and was avoided by ensuring the solution level remained well below the clips. In any case, out of the 19 wafers that did not display this problem, a total of 722 molecular devices were tested, with an overall yield of 99.4% (see table 1). Excluding one six-wafer run that produced devices that were not suitable for use in the clipping circuit due to instability, the remaining 13 wafers produced 494 devices overall, with 95.5% producing stable and useful clipping after all fabrication and packaging steps are finished. Overall, the yields achieved using these methods in a research-laboratory environment demonstrate the potential for economically feasible manufacturing of molecular electronic devices.

The variability of the current–voltage response of working devices from one batch was assessed by comparing 189 junctions from five wafers of a typical fabrication run (the sixth wafer produced short-circuits due to loss of potential control during electrochemical deposition as noted above, and 2 devices were omitted due to operator error, and two junctions on one die were tested). Figure 7 shows the results of this analysis, where current–voltage curves (A) and histograms of currents at +1 V (B) are shown with a comparison to a Gaussian function calculated using the average and standard deviation for the devices with current at +1 V below 750 μA (chosen based on the histogram). The fit of the data to a Gaussian function implies that the variation is random, with the shoulder at higher current value due to a systematic factor (e.g. geometry of the wafer). Using the base of the Gaussian in figure 7(C) lying between 250 and 750 μA and the previously

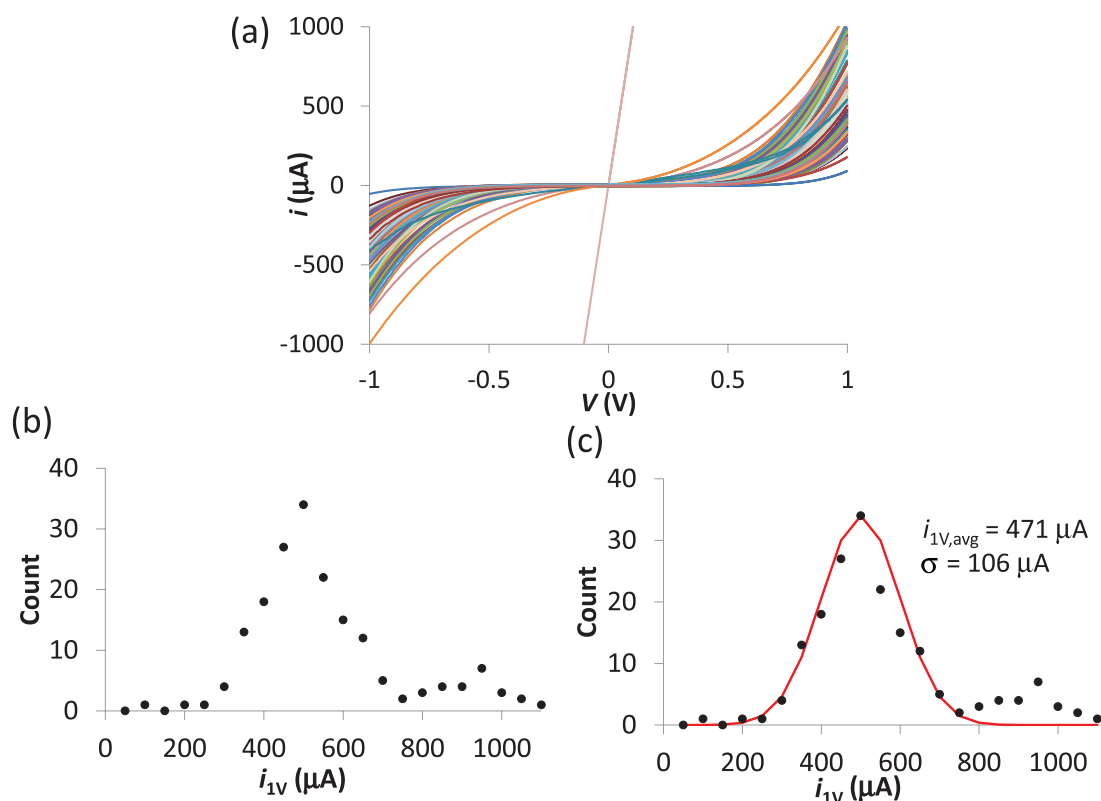


Figure 7. (A) Current–voltage curves for 180 molecular junctions fabricated across five wafers. (B) Histogram of the current measured at +1 V. (C) Comparison of the data set against a Gaussian function calculated using the average and standard deviation calculated for devices with current at +1 V less than 750 μA (the average and standard deviation for these is shown in the legend).

measured attenuation factor for carbon/molecule/carbon molecular devices [9] of 3.3 nm^{-1} , we estimate this spread in current can be explained by a thickness variation of $\sim 0.3 \text{ nm}$. Using the entire distribution, where the minimum current is $91 \mu\text{A}$, and the maximum is $1100 \mu\text{A}$, we obtain an estimate of 0.7 nm for the thickness difference that can account for the distribution. This level of variation is reasonable, and given that layer thicknesses in molecular junctions have been intentionally varied from 2 to 22 nm using diazonium chemistry [34], shows that an enormous range of behaviour is available using molecular electronics devices that can be made in a manufacturable manner.

The variability observed in the wafer-scale fabrication shown graphically in figure 7(A) is readily addressed by device selection and adjustments to the surrounding circuit elements and user controls. For example, the 180 devices illustrated in figure 7 are easily divided into ‘bins’ with narrow ranges of current response, and each ‘bin’ may be used for a particular type of music or distortion circuit. Given the wide range of distortion desired for different music genres, the variability in junction conductance may be an advantage not readily achieved with conventional semiconductors. It is also likely that fabrication refinements preceding commercial production will improve tolerances significantly, such that a narrow range of junction response can be achieved with high yield to serve a particular application. Since sound quality is subjective, we assessed user opinions about desirable ‘sounds’ by commissioning a professional guitarist to produce two YouTube videos which demonstrate MJ distortion circuits:

www.youtube.com/watch?v=9EJlihaLV9g
www.youtube.com/watch?v=arqzkv4w8yQ

Responses to these videos, and other feedback from a variety of professional and amateur players, has demonstrated that a wide range of junction sounds are desirable depending on the musical context and intent of the player. Additional user comments from early MJ distortion devices will be used to refine junction response for different genres and application, thus demonstrating the advantage of ‘tunability’ with structure and layer thickness inherent in molecular junctions. Finally, while other types of electronic devices with similar properties could be envisioned in audio clipping applications (e.g. inorganic tunnel junctions based on alumina [35]), a similar level of manufacturing must be achieved to be practical.

4. Conclusions

Collectively, the data presented here demonstrate that a molecular electronic device can serve in a real-world application: waveform clipping in electronic music processing circuits. The conventional, semiconductor components used up to this point have measurably and audibly different response compared to molecular junctions when used in audio clipping circuits (see the online supporting information for data correlation with sound samples (stacks.iop.org/JPhysCM/28/094011/mmedia)). We have shown that the difference in performance is derived from the electronic properties of the MJ, which result from different physics than those of

the pn junction. The distinct properties of MJs, pn-diodes, and vacuum tubes stem from their fundamentally different physical principles, and MJs should significantly increase the range of ‘sounds’ available in electronic music. Furthermore, the response of the circuit can be tuned by controlling the electronic properties of a single component, the MJ, during fabrication. In particular, the thickness of the molecular layer has an inverse exponential effect on its conductance, which allows the electronic properties of the molecular device to be tuned over a much more significant range than can be achieved with widely available semiconductor pn junction diodes or transistors. The harmonic distribution and sound quality of the MJ clipping circuit are similar to those resulting from vacuum tube amplifiers, with greatly reduced power and cooling requirements. We have also shown that molecular junctions can be manufactured reliably and reproducibly in a research laboratory setting, and that the level of variation resulting from parallel fabrication is well within what can reasonably serve the application. These factors demonstrate that a molecular junction in analog overdrive circuits provides previously unavailable and unique sounds characterized by softer clipping with milder harmonic distortion than conventional diode clippers. Thus, the use of molecular electronics in overdrive pedals should greatly expand the timbre palette available to musicians, and represents an application that has not yet been demonstrated with semiconductors. Given what is shown here, the future of molecular electronics looks bright—or perhaps more fittingly, sounds warm!

Acknowledgments

Additional data supporting this paper can be found in the online supplementary materials (stacks.iop.org/JPhysCM/28/094011/mmedia). This work was supported by the National Institute for Nanotechnology, which is operated as a partnership between the National Research Council, Canada, The University of Alberta, and the Government of Alberta. We would like to thank Daniel Pechanec for providing feedback and for the use of a tube amplifier. We thank Nick Jaffe (Just Nick Music) for outstanding feedback and an expertly delivered introduction to the guitar enthusiast community. Finally, we thank Ryan and Tanya Clarke of Dr Scientist Sounds for discussions, input, feedback, and the design and building of the prototypes. Adam Bergren and Richard McCreery declare that they have a developing commercial interest in the sale of molecular junctions.

References

- [1] Ratner M 2013 A brief history of molecular electronics *Nat. Nanotechnol.* **8** 378–81
- [2] Aviram A and Ratner M A 1974 Molecular rectifiers *Chem. Phys. Lett.* **29** 277–83
- [3] Salomon A, Cahen D, Lindsay S, Tomfohr J, Engelkes V B and Frisbie C D 2003 Comparison of electronic transport measurements on organic molecules *Adv. Mater.* **15** 1881–90
- [4] Heath J R 2009 Molecular electronics *Annu. Rev. Mater. Res.* **39** 1–23
- [5] McCreery R L and Bergren A J 2009 Progress with molecular electronic junctions: meeting experimental challenges in design and fabrication *Adv. Mater.* **21** 4303–22
- [6] Bard A J *et al* 2002 Charge transport through self-assembled monolayers of compounds of interest in molecular electronics *J. Am. Chem. Soc.* **124** 5550–60
- [7] Choi S H, Kim B and Frisbie C D 2008 Electrical resistance of long conjugated molecular wires *Science* **320** 1482–6
- [8] Akkerman H B, Blom P W M, de Leeuw D M and de Boer B 2006 Towards molecular electronics with large-area molecular junctions *Nature* **441** 69
- [9] Yan H, Bergren A J and McCreery R L 2011 All-carbon molecular tunnel junctions *J. Am. Chem. Soc.* **133** 19168–77
- [10] Moore G E 1965 Cramming more components onto integrated circuits *Electronics* **38** 114 (Republished in 1998 *Proc. IEEE* **86** 82–85)
- [11] Collier C P *et al* 1999 Electronically configurable molecular-based logic gates *Science* **285** 391–94
- [12] Kuekes P J, Williams R S and Heath J R 2003 *United States Patent* No. 6,128,214
- [13] Strukov D B, Snider G S, Stewart D R and Williams R S 2008 The missing memristor found *Nature* **453** 80–3
- [14] Kornilovich P, Bratkovski A M, Chang S-C and Williams R S 2003 *United States Patent* No. 6,670,631 B2
- [15] Metzger R M 2003 Unimolecular electrical rectifiers *Chem. Rev.* **103** 3803
- [16] Metzger R M 2006 Unimolecular rectifiers: present status *Chem. Phys.* **326** 176–87
- [17] Wassel R A, Credo G M, Fuierer R R, Feldheim D L and Gorman C B 2003 Attenuating negative differential resistance in an electroactive self-assembled monolayer-based junction *J. Am. Chem. Soc.* **126** 295–300
- [18] McCreery R, Yan H and Bergren A 2013 A critical perspective on molecular electronic junctions: there is plenty of room in the middle *Phys. Chem. Chem. Phys.* **15** 1065–81
- [19] Ru J, Szeto B, Bonifas A and McCreery R L 2010 Microfabrication and integration of diazonium-based aromatic molecular junctions *ACS Appl. Mater. Interfaces* **2** 3693–701
- [20] Gretarsson A M 2014 Scope software Prescott, AZ, USA <http://mercury.pr.erau.edu/~grea9a1/downloads/>
- [21] Hunter D 2013 *Guitar Effects Pedals: The Practical Handbook (Updated and Expanded Edition)* (Milwaukee, WI: Backbeat Books)
- [22] Hunter D 2005 *The Guitar Amp Handbook: Understanding Tube Amplifiers and Getting Great Sounds* (San Francisco, CA: Backbeat Books)
- [23] Pittman A 2003 *The Tube Amp Book* Deluxe revised edn (San Francisco, CA: Backbeat Books)
- [24] Yeh D T 2012 Automated physical modeling of nonlinear audio circuits for real-time audio effects: II. BJT and vacuum tube examples *IEEE Trans. Audio, Speech Lang. Process.* **20** 1207–16
- [25] Bergren A J, McCreery R L, Stoyanov S R, Gusarov S and Kovalenko A 2010 Electronic characteristics and charge transport mechanisms for large area aromatic molecular junctions *J. Phys. Chem. C* **114** 15806–15
- [26] Sayed S Y, Fereiro J A, Yan H, McCreery R L and Bergren A J 2012 Charge transport in molecular electronic junctions: compression of the molecular tunnel barrier in the strong coupling regime *Proc. Natl Acad. Sci. USA* **109** 11498–503
- [27] Sze S M 1981 *Physics of Semiconductor Devices* (New York: Wiley)
- [28] Akkerman H B *et al* 2007 Electron tunneling through alkanethiol self-assembled monolayers in large-area molecular junctions *Proc. Natl Acad. Sci. USA* **104** 11161–6

- [29] Van Hal P A *et al* 2008 Upscaling, integration and electrical characterization of molecular junctions *Nat. Nano* **3** 749–54
- [30] Mahmoud A M, Bergren A J, Pekas N and McCreery R L 2011 Towards integrated molecular electronic devices: characterization of molecular layer integrity during fabrication processes *Adv. Funct. Mater.* **21** 2273–81
- [31] Ranganathan S, McCreery R L, Majji S M and Madou M 2000 Photoresist-derived carbon for microelectrochemical applications *J. Electrochem. Soc.* **147** 277–82
- [32] Ranganathan S and McCreery R L 2001 Electroanalytical performance of carbon films with near-atomic flatness *Anal. Chem.* **73** 893–900
- [33] Anariba F, DuVall S H and McCreery R L 2003 Mono- and multilayer formation by diazonium reduction on carbon surfaces monitored with atomic force microscopy ‘scratching’ *Anal. Chem.* **75** 3837–44
- [34] Yan H *et al* 2013 Activationless charge transport across 4.5 to 22 nm in molecular electronic junctions *Proc. Natl Acad. Sci. USA* **110** 5326–30
- [35] Martin M-B *et al* 2014 Sub-nanometer atomic layer deposition for spintronics in magnetic tunnel junctions based on graphene spin-filtering membranes *ACS Nano* **8** 7890–5